arXiv:astro-ph/0209174v1 10 Sep 2002

Observed and Physical Properties of Core-Collapse Supernovae

Mario Hamuy[1]

The Observatories of the Carnegie Institution of Washington, 813 Santa Barbara Street, Pasadena, CA 91101

mhamuy@ociw.edu

ABSTRACT

I use photometry and spectroscopy data for 24 Type II plateau supernovae to examine their observed and physical properties. This dataset shows that these objects encompass a wide range of ∼5 mag in their plateau luminosities, their expansion velocities vary by ×5, and the nickel masses produced in these explosions go from 0.0016 to 0.26 $M_\odot$. From a subset of 16 objects I find that the explosion energies vary between 0.6× and 5.5×10^{51} ergs, the ejected masses encompass the range 14-56 $M_\odot$, and the progenitors' radii go from 80 to 600 $R_\odot$. Despite this great diversity several regularities emerge, which reveal that there is a continuum in the properties of these objects from the faint, low-energy, nickel-poor SNe 1997D and 1999br, to the bright, high-energy, nickel-rich SN 1992am. This study provides evidence that more massive progenitors produce more energetic explosions, thus suggesting that the outcome of the core collapse is somewhat determined by the envelope mass. I find also that supernovae with greater energies produce more nickel. Similar relationships appear to hold for Type Ib/c supernovae, which suggests that both Type II and Type Ib/c supernovae share the same core physics. When the whole sample of core collapse objects is considered, there is a continous distribution of energies below 8×10^{51} ergs. Far above in energy scale and nickel production lies the extreme hypernova 1998bw, the only supernova firmly associated to a GRB.

Subject headings: nucleosynthesis — supernovae : general

1. INTRODUCTION

The advent of new telescopes and better detectors is causing a rapid increase in the quality and quantity of observations obtained for supernovae (SNe, hereafter) of all types.

[1]Hubble Fellow

Although the field of Type Ia SNe (exploding white dwarfs) has developed considerably faster in recent years (due to the widely acknowledged importance of such objects as cosmological probes), there is a growing body of data for core collapse SNe. In this paper I collect all of the available data on hydrogen-rich plateau Type II SNe (those undergoing little interaction with the circumstellar medium, SNe II-P hereafter), with the purpose to better understand the nature of such objects.

I start in section 2 by summarizing the observational material available on 24 SNe II-P, after which (Sec. 3) I proceed to examine their great diversity and the correlations among the observed parameters. Using the hydrodynamic models of Litvinova & Nadezhin (1983, 1985, hereafter LN83, LN85) I go a step further and derive physical parameters (explosion energies, progenitor masses and radii) for 13 SNe II-P (Sec. 4). Although the statistics are still poor, this study shows that progenitors with greater masses produce more energetic explosions and synthesize more nickel. These correlations provide valuable clues and a better insight on the explosion mechanisms. In section 5 I combine the physical parameters of the SNe II-P with those previously published for SNe Ib/c. It appears that all core collapse SNe display the same correlations, which suggests that all of these objects share the same core physics. I discuss the properties of all core collapse SNe and how hypernovae fit in this group.

2. OBSERVATIONAL MATERIAL

Table 1 lists the 24 SNe II-P for which I have photometric and spectroscopic data. For each SN this table includes the heliocentric redshift (from the NASA/IPAC Extragalactic Database or my own measurement), reddening due to our own Galaxy (Schlegel, Finkbeiner, & Davis 1998), host galaxy extinction, the distance, and the method used to derive the distance.

In two cases I use Cepheid distances in the scale published by Ferrarese et al. (2000, F00). For five objects it is possible to assign the SN host galaxy to a galaxy group with surface brightness fluctuation (SBF) distances (Tonry et al. 2001) in the F00 Cepheid scale (adopting an uncertainty of 1 Mpc to account for cluster depth). For the 9 SNe which are not sufficiently far in the Hubble flow (cz<3000 km s^{-1}) and do not have SBF or Cepheid distances, it proves necessary to correct their observed redshifts in order to account for peculiar motions of their host galaxies. For this purpose I adopt the parametric model for peculiar flows of Tonry et al. (2000) which includes infall into Virgo and the Great Attractors, an overall dipole, and a cosmic thermal velocity dispersion of 187 km s^{-1}. Given the observed Cosmic Microwave Background (CMB) redshift the model yields a SBF distance in the F00

scale. For the 8 most distant objects with CMB redshifts greater than 3000 km s^{-1} I use their redshifts to compute the distances and an associated velocity dispersion of 187 km s^{-1}. To be consistent with the method employed for the nearby SNe, I adopt the best value for the Hubble constant in the F00 scale, namely, H_0=68±2 from SNe Ia (Gibson et al. 2000). Note however that the SBF distances in the F00 scale yield H_0=77±4 (Tonry et al. 2000), which suggests that the SBF and SN Ia distances could be systematically different (for a different view see Ajhar et al. (2001), who claim that the SBF and SNe Ia distances agree very well). For now I prefer to adopt H_0=68 since this value is determined from SNe Ia well in the quiet Hubble flow (unlike the value derived from SBF). Certainly, it would be more convenient to use the new Cepheid scale reported by the Hubble Space Telescope (HST) Key Project (Freedman et al. 2001) instead of the F00 scale since the new scale reconciles the SBF and SNe Ia methods, but it will necessary to wait until the parametric model for peculiar flows of Tonry et al. (2000) is updated.

The estimate of the amount of foreground visual extinction is under good control (σ=0.06 mag) thanks to the IR dust maps of Schlegel, Finkbeiner, & Davis (1998). The determination of absorption in the host galaxy, on the other hand, is more challenging. Since SNe II occur near HII regions, this is potentially a significant problem. To zero order SNe II-P should all reach the same temperature of hydrogen recombination during the plateau phase, so a measurement of the color should give directly the color excess due to dust absorption. Unfortunately, significant variations between 6,000-12,000 K are expected for the photosphere depending on the H/He abundance ratio (Arnett 1996) which limits the precision of the method to estimate color excesses. Keeping this caveat in mind, I proceed to use the observed colors to estimate $A_{host}(V)$ assuming that all SNe reach the same color at the end of the plateau. For this purpose I adopt the well-studied SN 1999em as the reference for the intrinsic color, and the $A_{host}(V)$=0.18 value derived by Baron et al. (2000) from detailed theoretical modeling of the spectra of SN 1999em. As Table 1 shows it, for 22 SNe it is possible to use their $B-V$ colors to derive extinction. A concerning problem with the $B-V$ method is that it yields negative reddenings for 10 SNe. This is particularly pronounced among the historical SNe, reaching $A_{host}(V)$=-1.2 for SN 1970G. It is possible that part of the problem is due to inadequate transformations of the photographic magnitudes into the standard Johnson system, or to background contamination by the host galaxy. However, even SN 1999cr (with modern CCD photometry) yields a negative value of $A_{host}(V)$=-0.75, which is well beyond the photometric errors. Perhaps this could be due to metallicity effects which are expected to be stronger in the B band where line blanketing is stronger. For 17 SNe I use their $V-I$ colors to derive an independent reddening estimate. This method is much well behaved: only SN 1992af yields a modest negative reddening of $A_{host}(V)$=-0.2. Ideally it would be more convenient to use the $V-I$ extinction values –

which are expected to be less sensitive to metallicity effects – but, since I do not have VI photometry for all SNe, in what follows I simply use the average of the $B-V$ and $V-I$ extinction values or the single-color value when only one color is available. I can estimate the uncertainties in $A_{host}(V)$ by comparing the difference in reddening yielded by both methods. Such differences amount to 0.46 mag on average, which implies a minimum error of 0.23 mag in the reddening estimate from an individual color. To be conservative I assume ± 0.3 mag in $A_{host}(V)$ for all SNe.

3. OBSERVED PARAMETERS FOR TYPE II SUPERNOVAE

Table 2 summarizes some observables that can be measured for the 24 SNe II including: the time of explosion (t_0) which comes from a Baade-Wesselink analysis and/or considerations about the discovery and pre-discovery image epochs; the observed V magnitude near the middle of the plateau (V_{50}); the corresponding absolute V magnitude corrected for extinction (M_{50}^V); the SN ejecta velocity near the middle of the plateau (v_{50}) measured from the minimum of the Fe II λ5169 line (corrected for host galaxy redshift) with an adopted uncertainty of 300 km s^{-1} for all SNe; the fiducial time (t_{50}) at which I measure V_{50} and v_{50} (arbitrarily chosen to be 50 rest-frame days after explosion); the characteristic V magnitude of the exponential tail (V_t); the time (t_t) at which I measure V_t; the nickel mass (M_{Ni}) produced in the explosion; and the specific data sources of photometry and spectroscopy.

Figure 1 shows a comparison between the SN plateau luminosities and their expansion velocities. The correlation between M_{50}^V and v_{50} is quite evident and proves similar to that previously reported by Hamuy & Pinto (2002) from a smaller sample of SNe II. This result reflects the fact that, while the explosion energy increases so do the kinetic and internal energies. This correlation implies that the SN luminosities can be standardized to a level of $\sim$0.3 mag from a spectroscopic measurement of the SN ejecta velocity. This method (named Standardized Candle Method, or SCM for short) suggests that SNe II-P have a potential utility as cosmological probes. A comparison of this empirical correlation to the 27 models of LN83 and LN85 can be seen in the top panel of Figure 2. Although there is reasonable agreement between observations and theory, the models (represented with crosses) show substantially greater scatter than the observed quantities. It must be pointed out, however, that several of the LN83 and LN85 calculations are for progenitors with less than 4 $M_\odot$, which seems unrealistically low (see section 4). When the sample of models is restricted to a more realistic subset of progenitor masses (≥ 8 $M_\odot$) the agreement is significantly better, as can be appreciated in the bottom panel of Figure 2. It is clear that the luminosity-velocity relation is also present in the theoretical calculations, although it seems that nature produces

a narrower correlation.

The nickel masses (M_{Ni}) listed in Table 2 are derived from the brightness of the SN exponential tails, assuming that all of the γ rays due to ^{56}Co $\rightarrow$ ^{56}Fe are fully thermalized (^{56}Co is the daughter of ^{56}Ni, which has a half life of only 6.1 days). This is a reasonable assumption given that most, if not all, SNe II-P have late-time decline rates consistent with ^{56}Co $\rightarrow$ ^{56}Fe. The first step in this calculation is the conversion of V_t into a bolometric luminosity which can be accomplished with the following formula,

$$log_{10}L_t \ = \ \frac{-[V_t \ - \ A_{GAL}(V) \ - \ A_{host}(V) \ + \ BC] \ + \ 5 \ log_{10}D \ - 8.14}{2.5}, \qquad (1)$$

where L_t is the tail luminosity (ergs s^{-1}), D is the distance in cm, BC is a bolometric correction that permits one to transform V magnitudes into bolometric magnitudes, and the additive constant provides the conversion from Vega magnitudes into cgs units. From SN 1987A and SN 1999em I found that BC=0.26$\pm$0.06 during the nebular phase (Hamuy 2001). Once the tail luminosity is computed the nickel mass can be found via,

$$M_{Ni} \ = 7.866 \times 10^{-44} \times L_t \times \ exp \left\{ \frac{(t_t - t_0)/(1+z) - 6.1}{111.26} \right\} M_{\odot}, \qquad (2)$$

where 6.1 is the half-life (in days) of ^{56}Ni and 111.26 is the e-folding time (in days) of the ^{56}Co decay, each of which releases 3.57 MeV in the form of γ rays (Woosley, Pinto, & Hartmann 1989). The nickel masses resulting from this method are given in Table 2 for 20 SNe, along with values independently derived for SN 1987A and SN 1997D by Arnett (1996) and Zampieri et al. (2002), respectively. The nickel masses of this sample show a remarkably wide range: while SN 1999br yielded only 0.0016 $M_{\odot}$, SN 1992am produced 0.26 $M_{\odot}$ of ^{56}Ni (in good agreement with the 0.3 $M_{\odot}$ value previously reported by Schmidt et al. (1994b)). This result is clearly inconsistent with previous claims that SNe II-P produce nearly the same amount of nickel (Hamuy & Suntzeff 1990; Patat et al. 1994), but in good agreement with more recent studies (Turatto et al. 1998; Sollerman 2002). Next I proceed to examine how M_{Ni} is related to the other observables.

In numerical simulations the shock wave generated by the collapse of the core propagates through the star's envelope, heating the material and triggering nuclear processing in the layers above the core where the temperatures are sufficiently high. Since the internal temperature is determined by the progenitor's radius (R_0) and the explosion energy (E) by the relation

$$T \approx \left[\frac{3E}{4\pi R_0^3 a}\right]^{1/4}, \tag{3}$$

the degree of nucleosynthesis is expected to be relatively greater for SNe with smaller progenitors and greater energies (Weaver & Woosley 1980), at least to zero order. In reality the physics is more complex, and the amount of observed nickel depends also on how much of the material located at the bottom of the envelope falls back to the newborn neutron star (or black hole). Theory as yet provides no physical constraints to this process and the amount of infalling material is freely adjusted via a "mass-cut" parameter. Since models currently offer no predictions on how the explosion parameters affect the degree of nucleosynthesis in core collapse SNe, observations can play an important role to placing constraints on the explosion mechanisms. This issue can be examined by comparing how the nickel mass produced in the explosion is related to the SN plateau properties (velocity and luminosity) which are determined by the explosion parameters (Arnett 1996; Popov 1993, LN83, LN85). Among the objects of the sample, SN 1992am is the one with the greatest nickel yield (0.26 $M_\odot$) and the brightest plateau (M_{50}^V=-18.57). On the other end, SN 1999br is characterized by a dim plateau (M_{50}^V=-13.32) and a small Ni production of only 0.0016 $M_\odot$. This pair of objects suggests that the plateau luminosity is correlated with the nickel mass. To examine this issue, Figure 3 shows M_{50}^V versus M_{Ni}. There is clear evidence that SNe with brighter plateaus produce more nickel. Since the plateau luminosities and velocities are tightly correlated (Fig. 1), it is expected that v_{50} is correlated with M_{Ni}. This is the case, indeed, as can be seen in Figure 4, where SN 1992am and SN 1999br again appear as extreme objects. Since the kinetic energy comprises 90% of the explosion energy of SNe II (Arnett 1996), this result suggests that SNe with greater explosion energies undergo more nuclear burning. It must be kept in kind, however, that not all SNe II-P necessarily eject the same mass, so it is possible that their expansion velocities do not provide a direct measure of their kinetic energies. In the next section I examine this point in more detail.

4. PHYSICAL PARAMETERS FOR TYPE II SUPERNOVAE

In an elegant paper Arnett (1980) derived analytic solutions for lightcurves of SNe II-P with the purpose to derive physical parameters for such objects. Using more realistic hydrodynamic models LN83 and LN85 derived approximate relations that connect the explosion energy (E), the mass of the envelope (M), and the progenitor radius (R_0) to three observable quantities, namely, the duration of the plateau, the absolute V magnitude, and the photospheric velocity observed in the middle of the plateau. These equations provide a simple and quick method to derive E, M, and R_0 from observations of SNe II-P without having to craft

specific models for each SN. A generalized analytic solution was subsequently worked out by Popov (1993), which proved in good agreement with the theoretical relations of Litvinova & Nadezhin (1985). So far these methods have been only applied to the one object (SN 1969L) which had sufficient observations for this analysis. In this section I revisit this issue based on a larger sample of SNe II-P, with the purpose to better understand the nature of such objects.

Of all the SNe II-P listed in Table 2 only 13 have sufficient data to apply the method of LN85. In the top section of Table 3 I list such objects and the observed quantities required for the LN85 analysis, in the following order: the time of explosion (t_0); the end of the plateau phase (t_p) defined as the time when the SN magnitude is near the mid-point between the plateau magnitude and that of the onset of the nebular phase; the plateau visual magnitude (V_p) measured at $t = (t_0 + t_p)/2$ (the middle of the plateau); and the SN ejecta velocity at the middle of the plateau (v_p) measured from the minimum of the Fe II λ5169 line [2]. Figure 5 shows the extinction-corrected absolute V-band lightcurves for the 13 SNe II-P and the end of the plateau phase for each SN.

With these data and the formulas given by LN85 I can solve now for E, M, and R_0. I attach 1-σ uncertainties to each of the parameters from Monte Carlo simulations in which I randomly vary the observed quantities according to the observational errors. The resulting parameters are summarized in Table 3. Also included in Table 3 is SN 1987A which was modeled in detail by Arnett (1996). Although SN 1987A showed an atypical lightcurve due to the compact nature of its blue supergiant progenitor, it was not fundamentally different than ordinary SNe II-P in the sense that it had a hydrogen-rich envelope at the time of explosion. For this reason I include it in this analysis. Also given in Table 3 are SN 1997D and SN 1999br, two low-luminosity SNe II-P recently modeled by Zampieri et al. (2002). To my knowledge these are the only 16 SNe with available physical parameters.

Among this sample, 9 SNe have explosion energies close to the canonical 1 foe value (1 foe=10^{51} ergs), 6 objects exceed 2 foes, and one has only 0.6 foes. SN 1992am and SN 1999br show the highest and lowest energies with 5.5 and 0.6 foes, respectively. This reveals that SNe II encompass a wide range in explosion energies. The ejected masses vary between 14 and 56 $M_\odot$. Although the uncertainties are large it is interesting to note that, while stars born with more than 8 $M_\odot$ can in principle undergo core collapse, they do not show up as SNe II-P. Perhaps they undergo significant mass loss before explosion and are observed as SNe II-n or SNe Ib/c. It proves interesting also that stars as massive as 50 $M_\odot$ seem able to retain a significant fraction of their H envelope and explode as SNe II. Objects with

[2]Note that V_p and v_p are close but not identical to the parameters V_{50} and v_{50} used in the section 3.

M>35 $M_\odot$ are supposed to lose their H envelope due to strong winds, and become Wolf-Rayet stars before exploding (Woosley, Langer, & Weaver 1993). This result suggests that stellar winds in massive stars are not so strong as previously thought, perhaps due to smaller metallicities. Except for four objects, the initial radii vary between 114 and 586 $R_\odot$. Within the error bars these values correspond to those measured for K and M red supergiants (van Belle et al. 1999), which lends support to the generally accepted view that the progenitors of SNe II-P have extended atmospheres at the time of explosion (Arnett 1996). Three of the SNe II-P of this sample, however, have R_0∼80 $R_\odot$ which corresponds to that of G supergiants. This is somewhat odd because such objects are not supposed to have plateau lightcurves but, instead, one like that of SN 1987A. Note, however, that the uncertainties are quite large and it is possible that these objects did explode as red supergiants.

Figure 6 shows M and M_{Ni} as a function of E for the 16 SNe II-P. Despite the large error bars, this figure reveals that a couple of correlations emerge from this analysis. The first interesting result (top panel) is that the explosion energy appears to be correlated with the envelope mass, in the sense that more massive progenitors produce higher energy SNe. This suggests that the outcome of the core collapse is somehow determined by the mass of the envelope. The second remarkable result (bottom panel) is that SNe with greater energies produce more nickel (a result already anticipated in section 3, and previously suggested by Blanton et al. (1995)). This could mean that greater temperatures and more nuclear burning are reached in such SNe, and/or that less mass falls back onto the neutron star/black hole in more energetic explosions.

Before leaving this section it is necessary to mention some caveats about these results:

• The LN85 formulas were obtained from models with progenitor masses and explosion energies below 2.9 $M_\odot$ and 16 foes, respectively. Clearly some of the SNe II-P in Table 3 lie outside the parameter space explored by LN85 and my results involve extrapolating their formulas. It will be necessary to expand the models to greater masses and energies before we can truly believe that SNe II-P have energies above 3 foes, progenitors with M∼50 $M_\odot$, and the correlations shown above.

• LN85 assumed that the plateau luminosity is fully powered by shock-deposited energy and they neglected a contribution by the ^{56}Co decay. It will be interesting to generalize the models in order to find out how the radioactive heating and the distribution of ^{56}Co affect the results presented here.

• In the LN85 models the plateau phase is preceded by a brief transient which lasts a few days, and the length of the plateau is measured from the time at which this short phase ends. The data for the 13 SNe do not show such transient, most likely because it is too

short, so I am forced to use the time of explosion for the beginning of the plateau. This should lead to an overestimate ($\sim$2%) of its length and a small bias in the derived physical parameters. Given the difficulty to measure the transient it would be desirable to re-derive the LN85 calibrations using a more operational definition of the onset of the plateau such as the explosion time.

• The LN85 formulas use the velocity of the photosphere (τ=2/3) as one of the input parameters. In my case I measure velocities from the minimum of the Fe II λ5169 line which is expected to arise just above the thermalization surface (the region where the radiation field forms). Since SNe II have electron scattering dominated atmospheres, the radiation field thermalizes well below the photosphere (Eastman, Schmidt, & Kirshner 1996) so that Fe II λ5169 should underestimate the photospheric velocity. In my thesis (Hamuy 2001) I examined this by measuring true photospheric velocities by cross-correlating (CC) the SN spectra with the Eastman et al. models. This study showed systematic differences between the Fe and CC velocities for individual objects but, curiously, no significant difference for the ensemble of SNe. This suggests that on average the Fe method is a good estimator of the photospheric velocity, although it may not work so well on an individual basis.

• To transform bolometric luminosities into V magnitudes LN65 employed bolometric corrections assuming that SNe II have blackbody spectra. SNe II are not perfect blackbodies, of course. Using the theoretical spectra of Eastman et al. I find that the bolometric corrections derived from Planck functions are $\sim$0.2 mag too large for $T_{eff}\geq$6500 K, about right ($\pm$0.1 mag) between 5000$\leq T_{eff}\leq$6500 K, and systematically low for $T_{eff}\leq$5000 K. It would be convenient that the LN65 formulas were re-derived with improved corrections.

5. PROPERTIES OF CORE COLLAPSE SUPERNOVAE

Core collapse SNe can also be hosted by massive stars which have lost most or all of their hydrogen-rich envelopes (SNe Ib), and even most or all of their helium envelopes (SNe Ic). It proves interesting therefore to compare the physical properties of such objects with those derived from SNe II-P. A bibliographic search reveals that there are only a handful well-studied SNe Ib/c. Table 4 lists such objects and the corresponding references from which their physical parameters were obtained.

In general, SNe Ib/c have bell-shaped lightcurves with a rise time of $\sim$15-20 days, a fast-decline phase of $\sim$30 days, and a slower decline phase at a rate between 0.01-0.03 mag day^{-1}. Unlike SNe II-P the lightcurves of SNe Ib/c are promptly powered by ^{56}Ni $\rightarrow$ ^{56}Co $\rightarrow$ ^{56}Fe. While the peak is determined by the amount of nickel synthesized in

the explosion, the width depends on the ability of the photons to diffuse out from the SN interior, which is determined by the envelope mass and expansion velocity. The early-time lightcurve, therefore, provides useful constraints on the ^{56}Ni mass, envelope mass, and kinetic energy (Arnett 1996). Additional constraints on the kinetic energy come from the Doppler broadening of the spectral lines. The late-time decline rate reveals that a fraction of the γ-rays from the radioactive decay escape from the SN ejecta without being thermalized and, therefore, can be used to quantify the degree of ^{56}Ni mixing in the SN interior. Nomoto and collaborators have modeled SNe Ib as helium stars that lose their hydrogen envelopes by mass transfer to a binary companion, and SNe Ic as C/O bare cores that lose their He envelope in a second stage of mass transfer. In both cases they assume spherically symmetric explosions. Table 4 summarizes the parameters derived from such models for the 7 SNe Ib/c.

Figure 7 shows envelope masses and nickel masses as a function of explosion energy for the seven SNe Ib/c along with the 16 SNe II shown in Figure 6. The top panel reveals that SNe Ib/c appear to follow the same pattern shown by SNe II, namely, that SNe with greater envelope masses produce more energetic explosions. The main difference between both subtypes, of course, is the vertical offset caused by the strong mass loss suffered by SNe Ib/c prior to explosion. From the bottom panel it is possible to appreciate that SN 1998bw was quite remarkable in explosion energy (60 foes) and nickel mass (0.5 $M_{\odot}$) compared to all of the other core collapse SNe. Owing to its extreme energy this object has been called hypernova. SN 1998bw is also remarkable because it was discovered at nearly the same place and time as GRB 980425 (Galama et al. 1998). The Type Ic SN 1997ef and SN 2002ap are located far below SN 1998bw in the energy scale (8 and 7 foes, respectively), yet far above the normal SN 1994I. Despite their greater than normal energies, neither of these objects produced unusually higher nickel masses compared to lower energy SNe Ib/c. Although the statistics are poor, it proves interesting that both SNe Ib/c and SNe II share the same location in this plane, which suggests that the core physics of both subtypes may not be fundamentally different.

When the whole sample of SNe II and SNe Ib/c is considered it seems that there is a continous distribution of energies below 8 foes. Within this regime it appears that SNe II can reach explosion energies comparable to that of the Type Ib/c SN 1997ef and SN 2002ap. Although the definition of hypernova is ambiguous, if SN 1997ef and SN 2002ap are included in this category (Nomoto et al. 2000; Mazzali et al. 2002), then at least one SN II (1992am) also qualifies as a hypernova. Whether the energy distribution is continuous above 8 foes remains to be seen when more data become available. This will permit us to understand if SN 1998bw belongs to a separate class of object or if it just lies at the extreme of the family of core collapse SNe. At the moment it is fair to say that there is only one firm supernovae/GRB association, and this object was clearly exceptional regarding energy and

nickel production within the SN context.

6. CONCLUSIONS

I assembled photometric and spectroscopic data for 24 SNe II-P which allowed me to draw the following conclusions,

1) As previously known, I recovered the result that SNe II-P encompass a wide range of ∼5 mag in plateau luminosities and a five-fold range in expansion velocities. I recovered the luminosity-velocity relation previously reported by Hamuy & Pinto (2002) which supports the claim that SNe II-P have a potential utility as cosmological probes. This empirical relation is also supported by the theoretical models of LN83 and LN85.

2) SNe II-P encompass a factor of 10 in nickel masses between 0.0016 (SN 1999br) and 0.26 $M_{\odot}$ (SN 1992am). There is clear evidence for a correlation in the sense that SNe with brighter plateaus and greater expansion velocities produce more nickel.

3) There is a continuum in the properties of SNe II-P from faint, low-velocity, nickel-poor events such as SN 1997D and SN 1999br, and bright, high-velocity, nickel-rich objects like SN 1992am. The correlations between plateau luminosities, expansion velocities, and nickel masses suggest that SNe II-P constitute a one parameter family.

4) Using the theoretical models of LN83 and LN85 I derived physical parameters for a subset of 13 SNe. Including SN 1987A, SN 1997D, and SN 1999br from previous studies I found that the explosion energies vary between 0.6 (SN 1999br) and 5.5 foes (SN 1992am), the ejected masses encompass the range 14-56 $M_{\odot}$, and the progenitors' radii go from 80 to 600 $R_{\odot}$.

5) Despite the large error bars, a couple of correlations emerge from the previous analysis: (1) more massive progenitors produce more energetic explosions, which suggests that the outcome of the core collapse is somewhat determined by the envelope mass; (2) SNe with greater energies produce more nickel. Similar relationships appear to hold for Type Ib/c SNe, which suggests that both Type II and Type Ib/c SNe share the same core physics.

I am grateful to Brian Schmidt for his thorough referee report, to John Tonry for sending me his code with the peculiar parametric flow model, and to Andrew McFayden for useful discussions during the preparation of this paper. I thank the Lorentz Center at Leiden University where I was able to complete a first draft of this paper. Support for this work was provided by NASA through Hubble Fellowship grant HST-HF-01139.01-A awarded by

the Space Telescope Science Institute, which is operated by the Association of Universities for Research in Astronomy, Inc., for NASA, under contract NAS 5-26555. This research has made use of the NASA/IPAC Extragalactic Database (NED), which is operated by the Jet Propulsion Laboratory, California Institute of Technology, under contract with the National Aeronautics and Space Administration. This research has made use of the SIMBAD database, operated at CDS, Strasbourg, France.

REFERENCES

Ajhar, E. A., Tonry, J. L., Blakeslee, J. P., Riess, A. G., & Schmidt, B. P. 2001, ApJ, 559, 584

Arnett, W. D. 1980, ApJ, 237, 541

Arnett, D. 1996, Supernovae and Nucleosynthesis, (New Jersey: Princeton Univ. Press)

Baron, E., et al. 2000, ApJ, 545, 444

Barbon, R., Ciatti, F., & Rosino, L. 1973, A&A, 29, 57

Benetti, S., Cappellaro, E., & Turatto, M. 1991, A&A, 247, 410

Benetti, S., Cappellaro, E., Turatto, M., Della Valle, M., Mazzali, P. A., & Gouiffes, C. 1994, A&A, 285, 147

Blanton, E. L., Schmidt, B. P., Kirshner, R. P., Ford, C. H., Chromey, F. R., & Herbst, W. 1995, AJ, 110, 2868

Cappellaro, E., Danziger, I. J., Della Valle, M., Gouiffes, C., & Turatto, M. 1995, A&A, 293, 723

Ciatti, F., Rosino, L., & Bertola, F. 1971, Mem. Soc. Ast. It., 42, 163

Ciatti, F., & Rosino, L. 1977, A&A, 56, 59

Clocchiatti, A., et al. 1996, AJ, 111, 1286

Eastman, R. G., Schmidt, B. P., & Kirshner, R. 1996, ApJ, 466, 911

Ferrarese, L., et al. 2000, ApJ, 529, 745

Freedman, W. L., et al. 2001, ApJ, 553, 47

Galama, T. J., et al. 1998, Nature, 395, 670

Gibson, B. K., et al. 2000, ApJ, 529, 723

Hamuy, M., & Suntzeff, N. B. 1990, AJ, 99, 1146

Hamuy, M. 2001, Ph.D. thesis, The University of Arizona

Hamuy, M., et al. 2001, ApJ, 558, 615

Hamuy, M., & Pinto, P. A. 2002, ApJ, 566, L63

Kirshner, R. P., & Kwan, J. 1974, ApJ, 193, 27

Leonard, D. C., et al. 2002a, PASP, 114, 35

Leonard, D. C., et al. 2002b, AJ, in press (astro-ph/0207601)

Litvinova, I. Y., & Nadezhin, D. K. 1983, Ap&SS, 89, 89

Litvinova, I. Y., & Nadezhin, D. K. 1985, SvAL, 11, 145

Mazzali, P. A., et al. 2002, ApJ, 572, 61

Nomoto, K., et al. 2000, in Gamma-ray Bursts, 5^{th} Huntsville Symposium, AIP Conf. Ser., Vol 526, ed. R. Marc Kippen, R. S. Mallozzi, & G. J. Fishman (New York: Melville), 622

Patat, F., Barbon, R., Cappellaro, E., & Turatto, M. 1994, A&A, 282, 731

Pennypacker, C. R., et al. 1989, AJ, 97, 186

Popov, D. V. 1993, ApJ, 414, 712

Pronik, V. I., Chuvaev, K. K., & Chugai, N. N. 1976, Sov. Ast. Letters, 20, 666

Ruiz-Lapuente, P., Kidger, M., Lopez, R., & Canal, R. 1990, AJ, 100, 782

Schlegel, D. J., Finkbeiner, D. P., & Davis, M. 1998, ApJ, 500, 525

Schmidt, B. P., et al. 1993, AJ, 105, 2236

Schmidt, B. P., Kirshner, R. P., Eastman, R. G., Phillips, M. M., Suntzeff, N. B., Hamuy, M., Maza, J., & Avilés, R. 1994a, ApJ, 432, 42

Schmidt, B. P., et al. 1994b, AJ, 107, 1444

Shigeyama, T., Nomoto, K., Tsujimoto, T., & Hashimoto, M. 1990, ApJ, 361, L23

Sollerman, J. 2002, New Astronomy Reviews, 46, 493

Tonry, J. L., Blakeslee, J. P., Ajhar, E. A., & Dressler, A. 2000, ApJ, 530, 625

Tonry, J. L., Dressler, A. D., Blakeslee, J. P., Ajhar, E. A., Fletcher, A. B., Luppino, G. A., Metzger, M. R., & Moore, C. B. 2001, ApJ, 546, 681

Tsvetkov, D. Y. 1988, Astrofizika, 29, 260

Tsvetkov, D. Y. 1994, Ast. Let., 20, 374

Turatto, M., Cappellaro, E., Benetti, S., & Danziger, I. J. 1993, MNRAS, 265, 471

Turatto, M., et al. 1998, ApJ, 498, L129

van Belle, G. T., et al. 1999, AJ, 117, 521

Weaver, T. A., & Woosley, S. E. 1980, in Proceedings of Texas Symposium on Relativistic Astrophysics, 9th, (New York: New York Acad. Sci.), 335

Winzer, J. E. 1974, Royal Astron. Soc. Canada Journal, 68, 36

Wood, R., & Andrews, J. 1974, MNRAS, 167, 13

Woosley, S. E., Pinto, P. A., & Hartmann, D. 1989, ApJ, 346, 395

Woosley, S. E., Langer, N., & Weaver, T. A. 1993, ApJ, 411, 823

Zampieri, L., Pastorello, A., Turatto, M., Cappellaro, E., Benetti, S., Altavilla, G., Mazzali, P., & Hamuy, M. 2002, MNRAS, submitted

This preprint was prepared with the AAS LaTeX macros v5.0.

Table 1. General Data for Type II Supernovae

SN	cz_{helio} ($km\ s^{-1}$)	Redshift Source	$A_{GAL}(V)$ ± 0.06	$A_{host}(V)$ $B-V$	$A_{host}(V)$ $V-I$	$A_{host}(V)$ ± 0.3	Distance (Mpc)	Distance Method
1968L	516	2	0.219	-0.90	···	0.00	4.1(1.0)	SBF (Cen A Group)
1969L	518	2	0.205	-0.70	···	0.00	10.0(1.0)	SBF (N1023 Group)
1970G	241	2	0.028	-1.20	···	0.00	7.4(0.3)	Cepheids
1973R	727	2	0.107	1.40	···	1.40	10.3(0.8)	Cepheids
1986I	2407	2	0.129	···	0.20	0.20	17.0(1.0)	SBF (Virgo Group)
1986L	1292	2	0.099	0.30	···	0.30	18.7(2.4)	SBF model
1988A	1519	2	0.136	-0.40	···	0.00	17.0(1.0)	SBF (Virgo Group)
1989L	1313	2	0.123	-0.60	0.90	0.15	17.0(2.4)	SBF model
1990E	1241	2	0.082	1.00	1.90	1.45	18.2(2.4)	SBF model
1990K	1584	2	0.047	0.05	0.35	0.20	23.2(2.4)	SBF model
1991al	4572	1	0.168	-0.30	0.10	0.00	65.9(2.4)	Redshift
1991G	757	2	0.065	···	0.00	0.00	14.7(1.0)	SBF (U Ma Group)
1992H	1793	2	0.054	0.00	···	0.00	29.4(2.4)	SBF model
1992af	5611	1	0.171	-0.40	-0.20	0.00	80.0(2.4)	Redshift
1992am	14310	2	0.164	0.35	0.20	0.28	206.0(2.4)	Redshift
1992ba	1104	2	0.193	-0.15	0.15	0.00	15.2(2.4)	SBF model
1993A	8790	1	0.572	0.00	0.10	0.05	131.4(2.4)	Redshift
1993S	9896	2	0.054	1.00	0.40	0.70	141.9(2.4)	Redshift
1999br	969	2	0.078	0.50	0.80	0.65	10.8(2.4)	SBF model
1999ca	2791	2	0.361	0.85	0.50	0.68	45.7(2.4)	Redshift
1999cr	6069	1	0.324	-0.75	0.10	0.00	93.8(2.4)	Redshift
1999eg	6703	2	0.388	-0.15	0.05	0.00	95.5(2.4)	Redshift
1999em	717	2	0.130	0.18	0.18	0.18	10.7(2.4)	SBF model
1999gi	592	2	0.055	0.50	0.85	0.68	9.0(2.4)	SBF model

References. — (1) Hamuy (2001); (2) NASA/IPAC Extragalactic Database.

Table 2. Observed Parameters for Type II Supernovae

SN	t_0 (JD - 2,400,000)	V_{50}	M_{50}^V	v_{50} ($\pm 300\ km\ s^{-1}$)	t_{50} (JD - 2,400,000)	V_t	t_t (JD - 2,400,000)	M_{Ni} ($M_\odot$)	Phot. Source	Spec. Source
1968L	40039.5(5)	12.03(08)	-16.25(55)	4020	40089.6	···	···	···	1	1
1969L	40550.5(5)	13.35(06)	-16.85(37)	4841	40600.6	17.16(10)	40860.0	$0.082^{+0.034}_{-0.026}$	2	2,3
1970G	40768.5(30)	12.10(15)	-17.27(35)	5041	40818.5	16.25(10)	40979.5	$0.037^{+0.019}_{-0.012}$	4,5	3,6
1973R	42008.5(15)	14.56(05)	-17.01(35)	5092	42058.6	17.23(28)	42187.8	$0.084^{+0.044}_{-0.030}$	7	7
1986I	46563.3(4)	14.55(20)	-16.93(34)	3623	46613.7	16.93(06)	46758.0	$0.117^{+0.039}_{-0.031}$	8,9	8
1986L	46707.9(4)	14.57(05)	-17.19(41)	4150	46758.1	18.16(15)	46864.1	$0.034^{+0.018}_{-0.011}$	10	10
1987A	···	···	···	···	···	···	···	0.075^a	···	···
1988A	47163.0(7)	15.00(05)	-16.29(34)	4613	47213.3	19.11(24)	47531.6	$0.062^{+0.029}_{-0.020}$	11,12,13	13,14
1989L	47650.0(15)	15.47(05)	-15.96(43)	3529	47700.2	18.67(12)	47796.7	$0.015^{+0.008}_{-0.005}$	15	16
1990E	47932.6(5)	15.90(20)	-16.93(43)	5324	47982.8	19.59(25)	48191.2	$0.062^{+0.031}_{-0.022}$	17,18	17,14
1990K	47970.0(30)	14.50(20)	-17.57(45)	6142	48020.3	18.84(07)	48178.6	$0.039^{+0.022}_{-0.014}$	19,20	14
1991al	48410.0(30)	16.62(05)	-17.64(34)	7330	48460.8	19.44(08)	48555.5	$0.095^{+0.048}_{-0.028}$	14	14
1991G	48280.0(5)	15.53(07)	-15.37(33)	3347	48330.1	17.69(03)	48428.0	$0.022^{+0.008}_{-0.006}$	21	21
1992H	48661.0(10)	14.99(04)	-17.41(36)	5463	48711.3	18.58(06)	48943.2	$0.129^{+0.053}_{-0.037}$	22,23	23
1992af	48736.0(30)	17.06(20)	-17.63(37)	5322	48786.9	19.42(03)	48891.6	$0.156^{+0.078}_{-0.051}$	14	14
1992am	48778.1(11)	18.44(05)	-18.57(31)	7868	48830.5	21.60(10)	48979.7	$0.256^{+0.099}_{-0.070}$	14	14
1992ba	48883.2(5)	15.43(05)	-15.67(43)	3523	48933.4	18.55(05)	49081.6	$0.019^{+0.009}_{-0.007}$	14	14
1993A	48985.5(10)	19.64(05)	-16.57(33)	4290	49037.0	···	···	···	14	14
1993S	49130.0(10)	18.96(05)	-17.55(30)	4569	49181.6	···	···	···	14	14
1997D	···	···	···	···	···	···	···	0.006^b	···	···
1999br	51277.9(3)	17.58(05)	-13.32(53)	1545	51328.1	22.68(08)	51643.7	$0.0016^{+0.0011}_{-0.0008}$	14,24	14
1999ca	51280.0(10)	16.65(05)	-17.69(35)	5353	51330.5	21.10(10)	51484.8	$0.038^{+0.017}_{-0.010}$	14	14
1999cr	51221.5(10)	18.33(05)	-16.86(29)	4389	51272.5	20.29(20)	51353.5	$0.090^{+0.034}_{-0.027}$	14	14
1999eg	51437.2(8)	18.65(05)	-16.64(31)	4012	51488.3	···	···	···	14	14
1999em	51474.0(3)	13.98(05)	-16.48(52)	3757	51524.1	16.70(03)	51636.8	$0.042^{+0.027}_{-0.019}$	25,26	25,27
1999gi	51518.2(3)	14.91(05)	-15.60(58)	3617	51568.3	17.62(05)	51676.6	$0.018^{+0.013}_{-0.009}$	28	28

[a]From Arnett (1996)

[b]From Zampieri et al. (2002)

References. — (1) Wood & Andrews (1974); (2) Ciatti, Rosino, & Bertola (1971); (3) Kirshner & Kwan (1974); (4) Winzer (1974); (5) Barbon, Ciatti, & Rosino (1973); (6) Pronik, Chuvaev, & Chugai (1976); (7) Ciatti & Rosino (1977); (8) Pennypacker et al. (1989); (9) Tsvetkov (1988); (10) M. M. Phillips & S. Kirhakos (2000) (private communication); (11) Ruiz-Lapuente et al. (1990); (12) Benetti, Cappellaro, & Turatto (1991); (13) Turatto et al. (1993); (14) Hamuy (2001); (15) B. Schmidt (2002) (private communication); (16) Schmidt et al. (1994a); (17) Schmidt et al. (1993); (18) Benetti et al. (1994); (19) Cappellaro et al. (1995); (20) M. M. Phillips (2000) (private communication); (21) Blanton et al. (1995); (22) Tsvetkov (1994); (23) Clocchiatti et al. (1996); (24) A. Pastorello & L. Zampieri (2002) (private communication); (25) Hamuy et al. (2001); (26) N. B. Suntzeff (private communication); (27) Leonard et al. (2002a); (28) Leonard et al. (2002b) .

Table 3. Observed and Physical Parameters for Type II Supernovae

SN	t_0 (JD - 2,400,000)	t_p (JD - 2,400,000)	V_p	v_p (± 300 km s^{-1})	Energy (10^{51} ergs)	Ejected Mass ($M_\odot$)	Initial Radius ($R_\odot$)	References
1969L	40550.5(5)	40660.0(7)	13.34(06)	4562	$2.3^{+0.7}_{-0.6}$	28^{+11}_{-8}	204^{+150}_{-88}	1
1973R	42008.5(15)	42119.0(7)	14.61(05)	4823	$2.7^{+1.2}_{-0.9}$	31^{+16}_{-12}	197^{+128}_{-78}	1
1986L	46707.9(4)	46813.0(7)	14.64(05)	4037	$1.3^{+0.5}_{-0.3}$	17^{+7}_{-5}	417^{+304}_{-193}	1
1988A	47163.0(7)	47305.0(35)	15.04(05)	3537	$2.2^{+1.7}_{-1.2}$	50^{+46}_{-30}	138^{+80}_{-42}	1
1989L	47650.0(15)	47790.7(7)	15.68(05)	2800	$1.2^{+0.6}_{-0.5}$	41^{+22}_{-15}	136^{+118}_{-65}	1
1990E	47932.6(5)	48063.9(10)	16.00(20)	4552	$3.4^{+1.3}_{-1.0}$	48^{+22}_{-15}	162^{+148}_{-78}	1
1991G	48280.0(5)	48403.0(7)	15.61(07)	3030	$1.3^{+0.9}_{-0.6}$	41^{+19}_{-16}	70^{+73}_{-31}	1
1992H	48661.0(10)	48777.5(10)	15.07(04)	5084	$3.1^{+1.3}_{-1.0}$	32^{+16}_{-11}	261^{+177}_{-103}	1
1992am	48778.1(11)	48951.1(29)	18.78(05)	5097	$5.5^{+3.0}_{-2.1}$	56^{+40}_{-24}	586^{+341}_{-212}	1
1992ba	48883.2(5)	49015.3(7)	15.56(05)	2954	$1.3^{+0.5}_{-0.4}$	42^{+17}_{-13}	96^{+100}_{-45}	1
1999cr	51221.5(10)	51347.5(10)	18.50(05)	3858	$1.9^{+0.8}_{-0.6}$	32^{+14}_{-12}	224^{+136}_{-81}	1
1999em	51474.0(3)	51598.0(5)	14.02(05)	3290	$1.2^{+0.6}_{-0.3}$	27^{+14}_{-8}	249^{+243}_{-150}	1
1999gi	51474.0(3)	51645.0(5)	14.98(05)	3168	$1.5^{+0.7}_{-0.5}$	43^{+24}_{-14}	81^{+110}_{-51}	1
Supernovae From Other Sources								
1987A	···	···	···	···	1.7	15	42.8	2
1997D	···	···	···	···	0.9	17	128.6	3
1999br	···	···	···	···	0.6	14	114.3	3

References. — (1) This paper; (2) Arnett (1996); (3) Zampieri et al. (2002) .

Table 4. Physical Parameters for Type Ib/c Supernovae

SN	Type	Energy (10^{51} ergs)	Ejected Mass ($M_\odot$)	Nickel Mass ($M_\odot$)	References
1983I	Ic	1.0	2.1	0.15	1
1983N	Ib	1.0	2.7	0.15	1
1984L	Ib	1.0	4.4	0.15	1
1994I	Ic	1.0	0.9	0.07	2
1997ef	Ic	8.0	7.6	0.15	2
1998bw	Ic	60.0	10.0	0.50	2
2002ap	Ic	7.0	3.75	0.07	3

References. — (1) Shigeyama et al. (1990); (2) Nomoto et al. (2000); (3) Mazzali et al. (2002) .

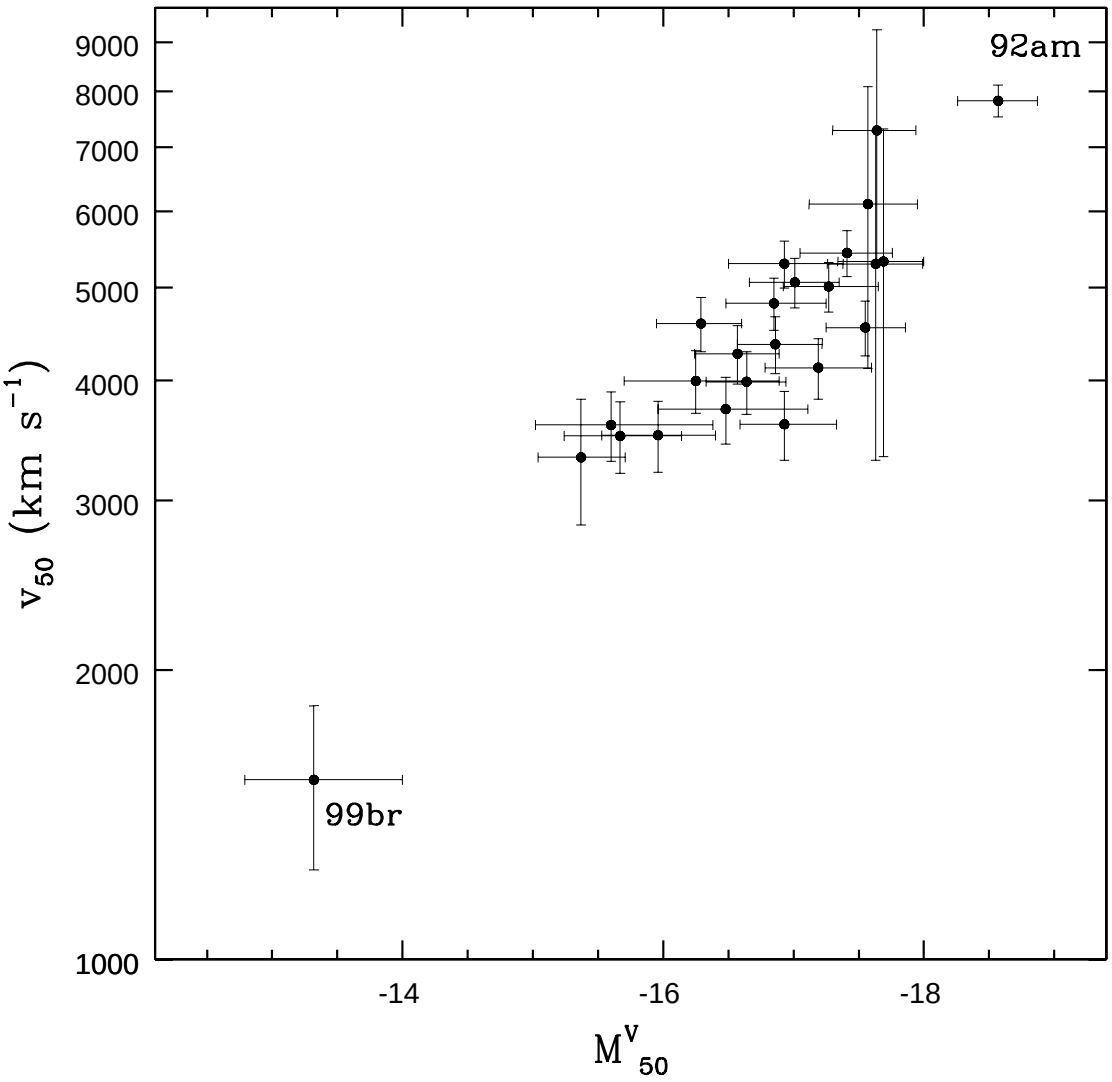

Fig. 1.— Expansion velocities from Fe II λ5169 versus absolute V magnitude, both measured in the middle of the plateau (day 50) of 24 SNe II-P.

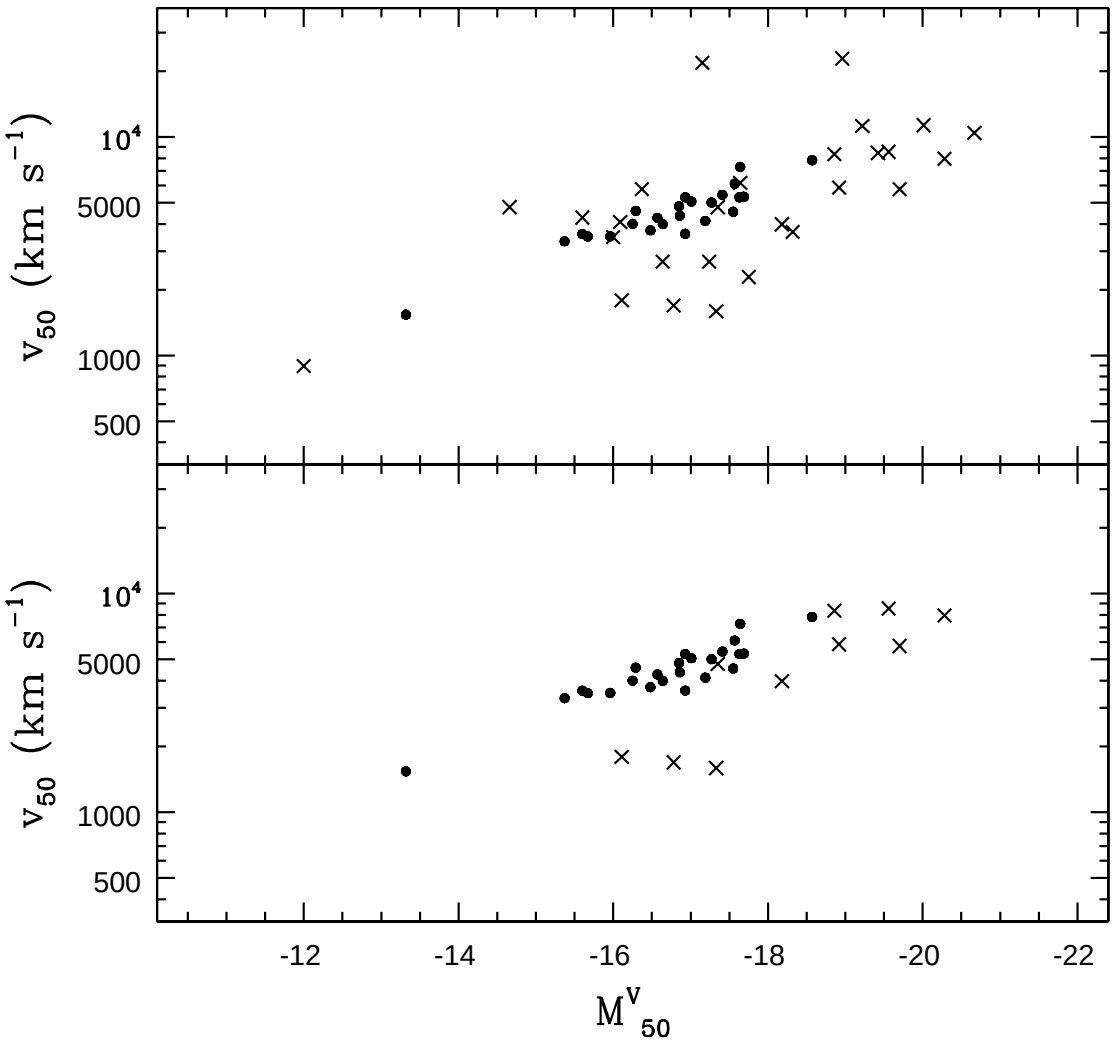

Fig. 2.— (top) Luminosity-velocity relation for 24 SNe II-P (solid points) and the 27 models of LN83 and LN85 (crosses). (bottom) Same as above, but for a restricted set of models with $\geq 8\ M_\odot$.

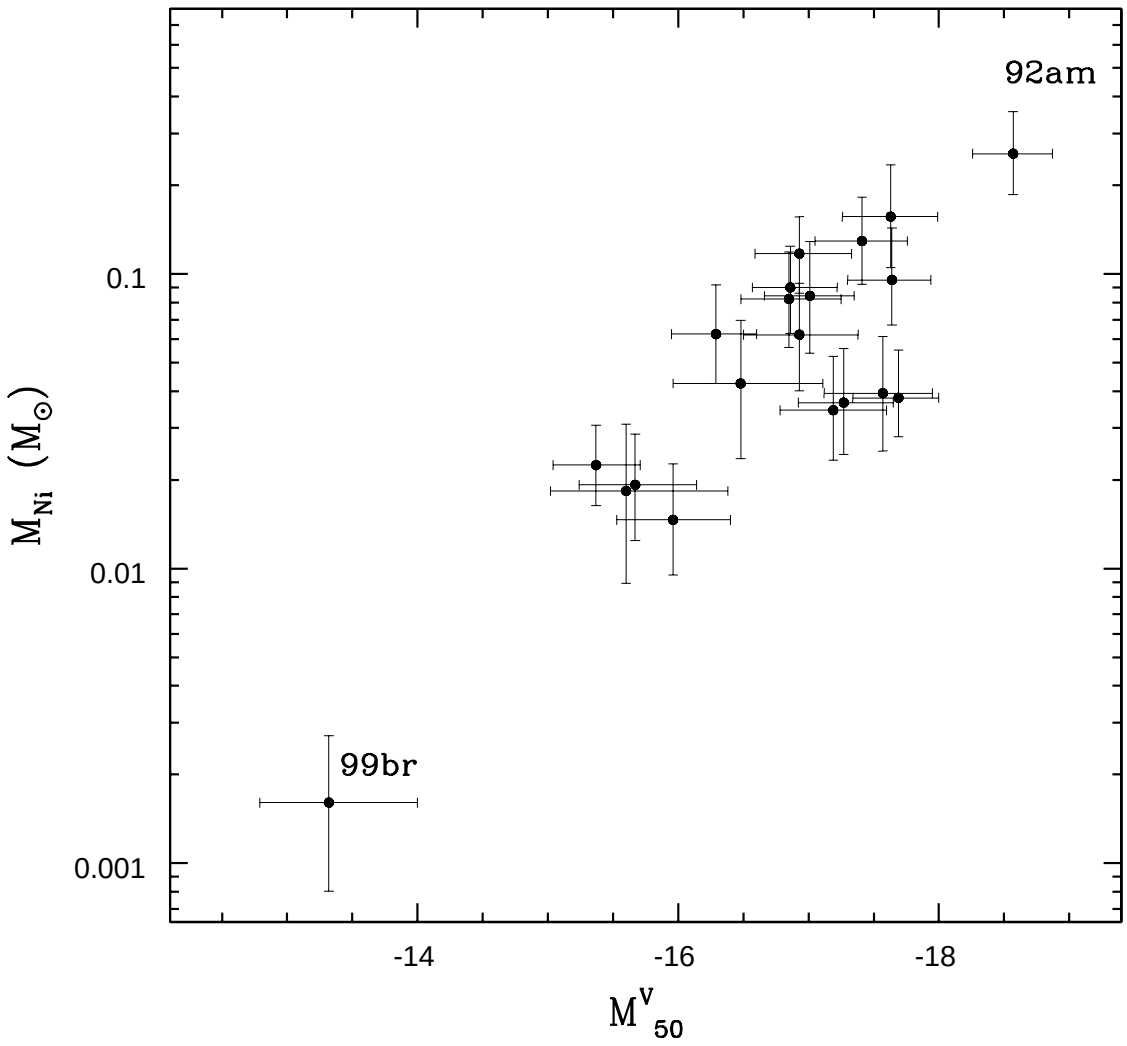

Fig. 3.— Mass of freshly synthesized ^{56}Ni versus plateau luminosity measured 50 days after explosion.

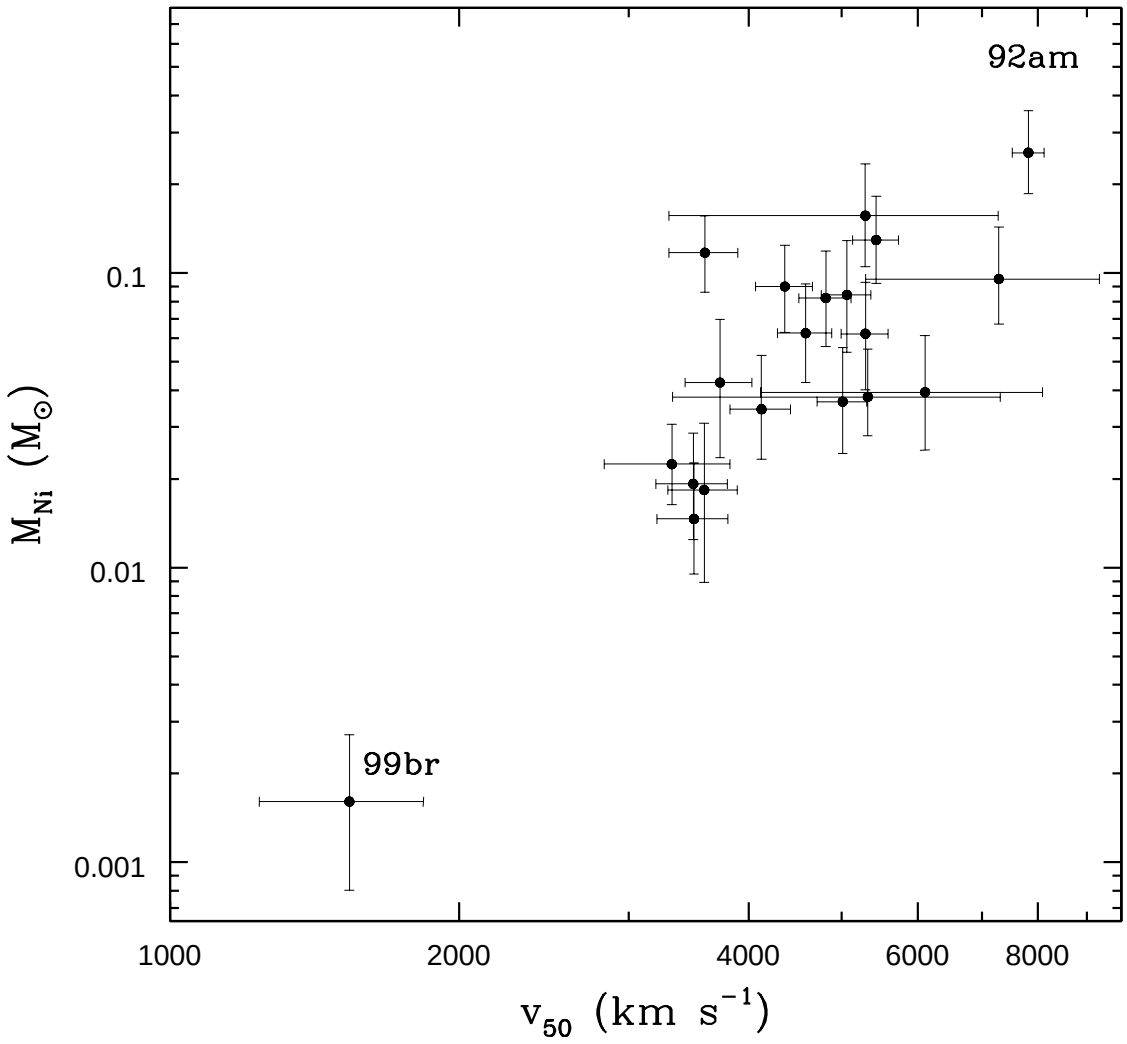

Fig. 4.— Mass of freshly synthesized ^{56}Ni versus expansion velocities measured from Fe II λ5169 in the middle of the plateau (day 50).

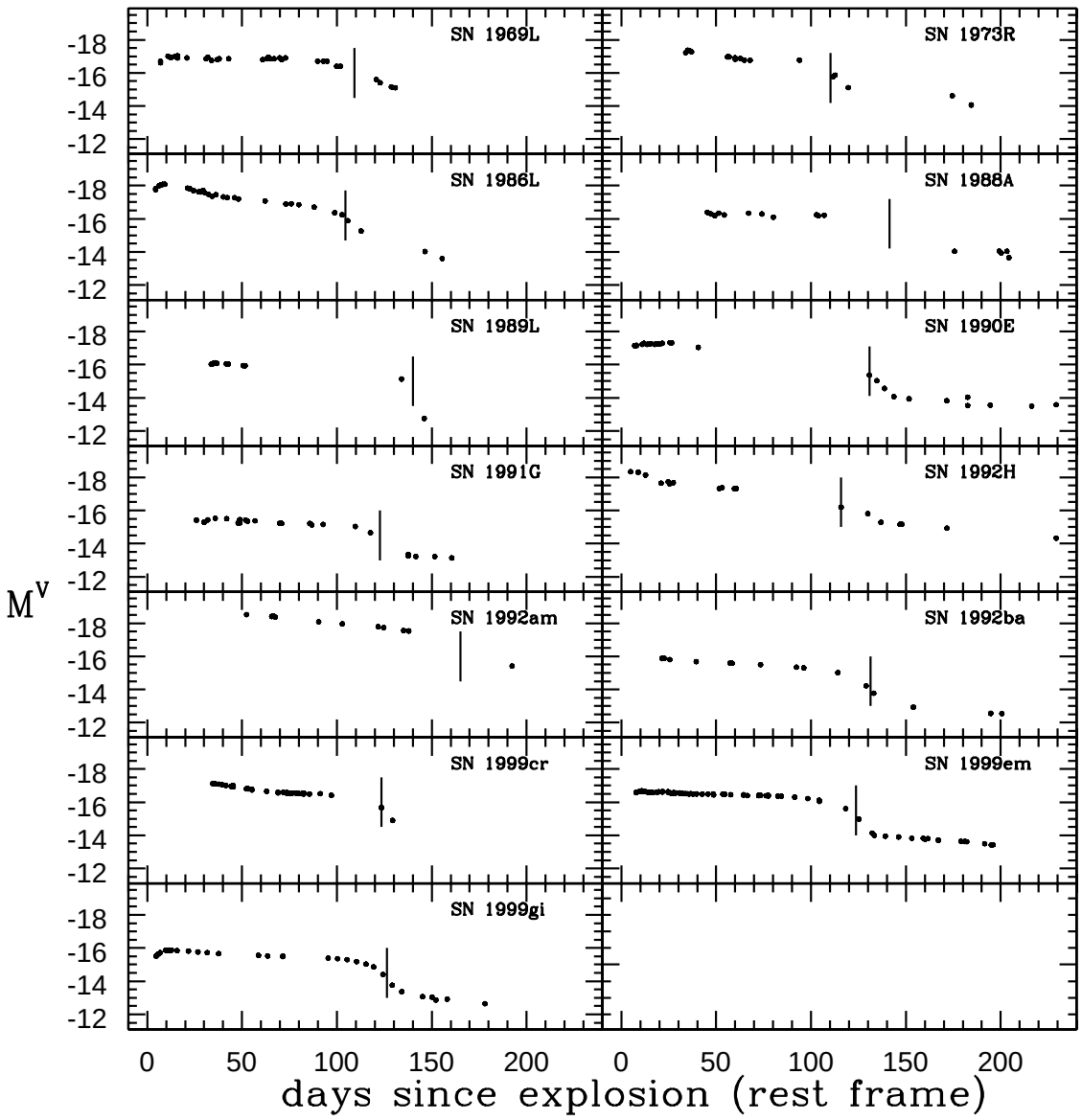

Fig. 5.— Extinction corrected absolute V-band lightcurves of the 13 plateau SNe II. The vertical bars indicate the end of the plateau phase for each supernova.

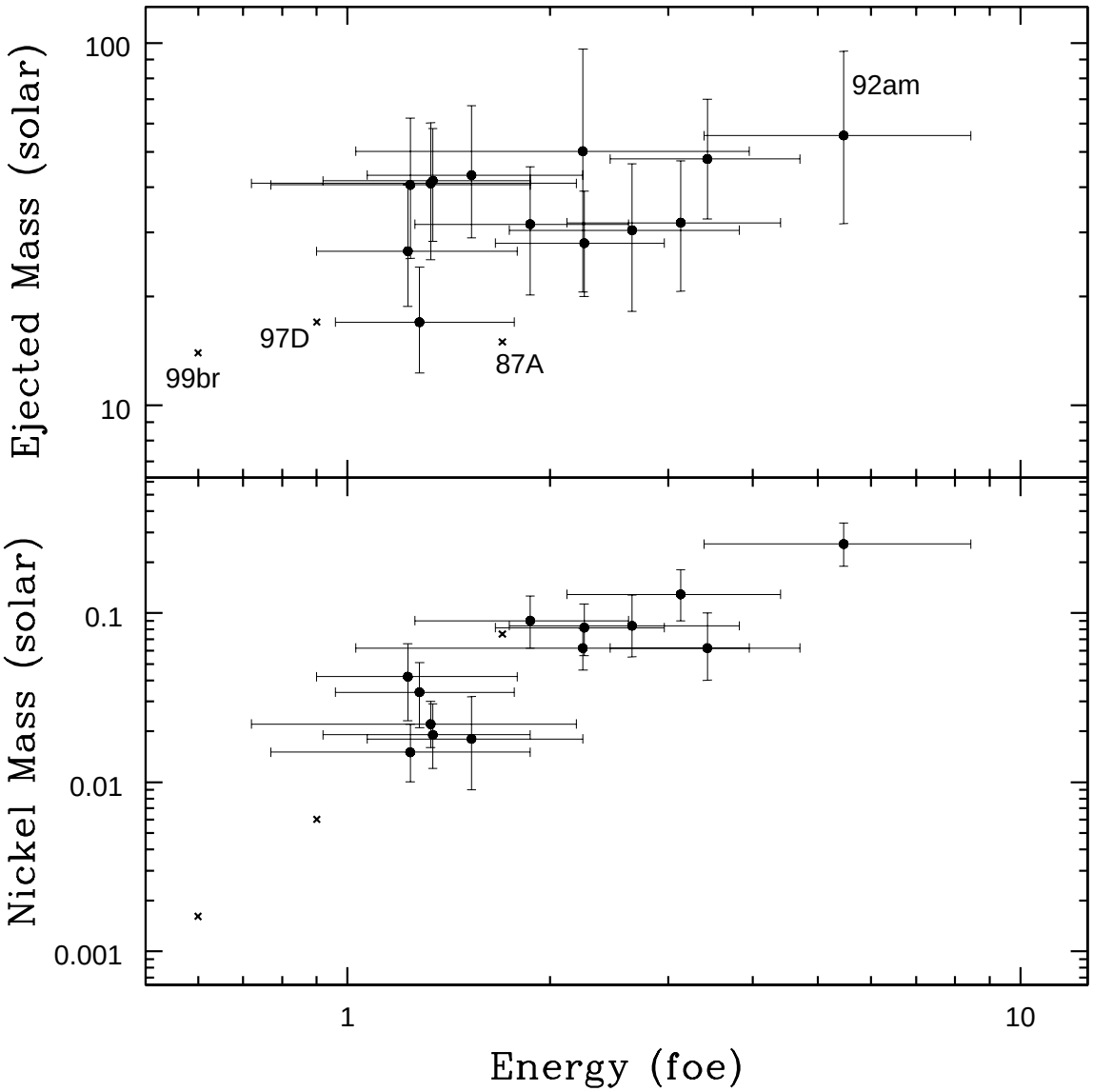

Fig. 6.— Envelope mass and nickel mass of SNe II, as a function of explosion energy. Solid points represent the 13 SNe II-P for which I was able to apply the technique of Litvinova & Nadezhin (1985). The three crosses correspond to SN 1987A, SN 1997D, and SN 1999br which have been modeled in detail by Arnett (1996) and Zampieri et al. (2002). The nickel yield for SN 1999br comes from this paper (Table 2).

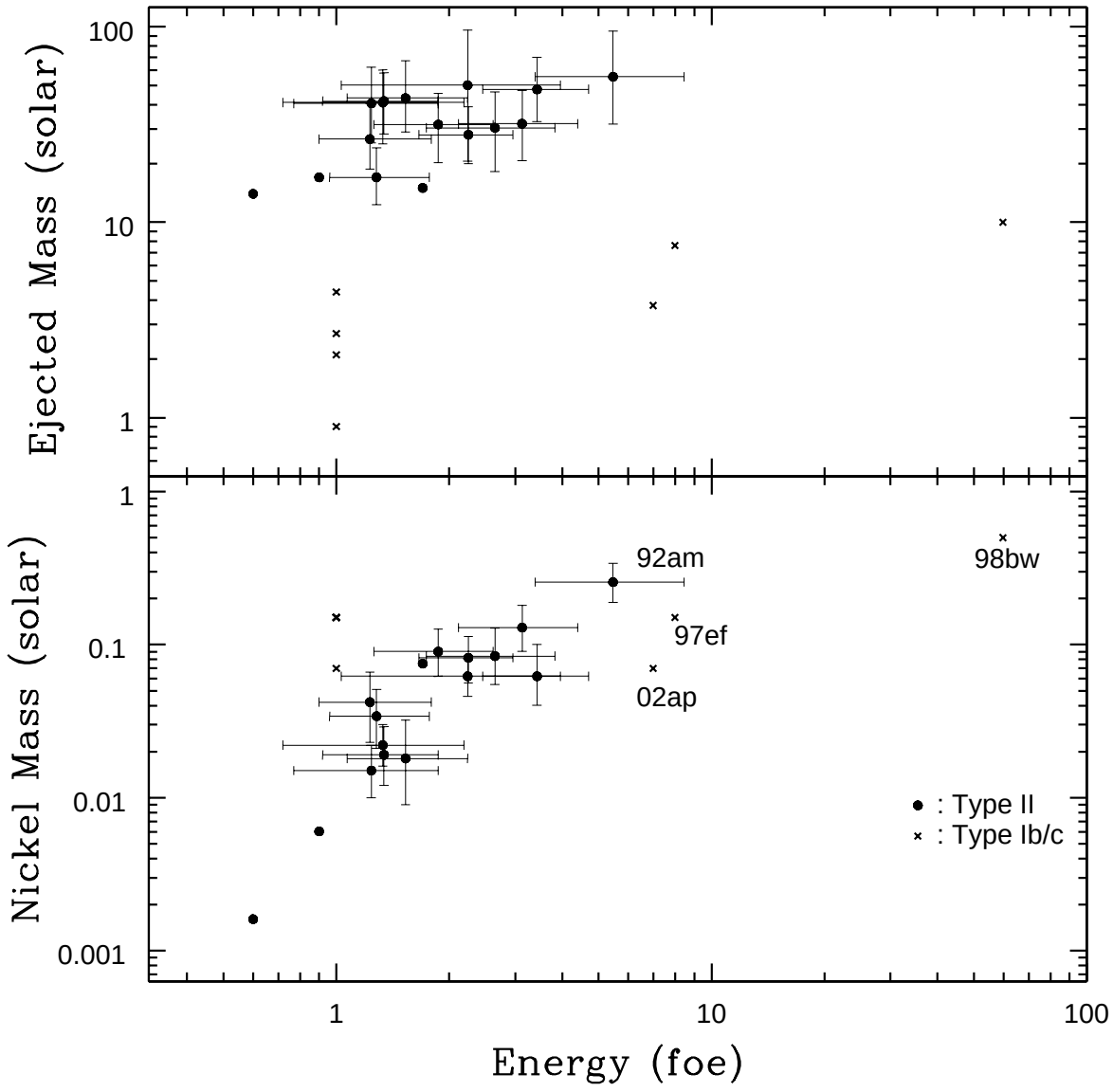

Fig. 7.— Envelope mass and nickel mass of core collapse SNe, as a function of explosion energy. Solid points are the same 16 SNe II shown in Figure 6, and crosses correspond to the 7 Type Ib/c SNe listed in Table 4.